IJP

Structural and optical properties of nanostructured PbS thin films chemically deposited at room temperature

A U Ubale*, R B Mankar, A S Daryapurkar, R R Raut and V S Sangawar

Thin Film Physics Laboratory, Department of Physics,
Govt Vidarbha Institute of Science and Humanities,
Amravati-444 604, Maharashtra, India

E-mail   ashokuu @yahoo com

Abstract   Nanostructured PbS thin films were deposited on to glass, by a chemical deposition method, Successive Ionic Layer Adsorption and Reaction (SILAR) at room temperature For deposition of PbS thin films, lead acetate was used as cationic and thioacetamide as anionic precursor in aqueous medium The structure and surface morphology of the films were characterized by X-ray diffraction and Scanning electron microscopy The optical investigation showed that depending on thickness, films have direct allowed transitions in the range 1 86-2 36 eV   The decrease in dc dark resistivity with increase in grain size was also examined

Keywords   Nanostructured thin film, PbS, SILAR method

PACS Nos.   61.10 Nz, 68 55 Jk and 81 55 Gh

1. Introduction

Nanostructured thin films have attracted the attention of an increasing number of researchers from several disciplines in the last ten years due to their outstanding electronic and optical properties and extensively useful applications in various optoelectronic devices. [1,2]. The small size of nanoparticles, which is responsible for the different properties (electronic, optical, electrical, magnetic and mechanical) of nanoparticles and nanostructured materials with respect to the bulk material, makes them suitable for new applications. The lead chalcogenide thin films are widely used in infrared detecting devices, diode lasers, humidity and temperature sensors and in solar control coatings [3-6].

Corresponding Author

Different workers have reported chemical deposition of PbS on different types of substrates with characterization [7-11]. Acharya and Bose [12] used lead acetate and thiourea to grow polycrystalline PbS thin films at 303 K. Nair and Nair [13] have deposited PbS films at 302 K from a bath containing Pb^{+2} ions and thiourea in the 1:3 molar ratio. Sharma et al [14] have studied effect of Cu doping on crystallite size and carrier density of PbS thin films. The SILAR technique is relatively new and less investigated method, first reported in 1987 by Ristov *et al* [15]. Nicolau ascribed the name SILAR to this technique in 1985[16,17]. SILAR and Chemical Bath Deposition (CBD) [18] techniques are based on successive adsorption and reaction of species on the substrate surface from aqueous solutions. In the present paper, an attempt has been made to deposit nanocrystalline PbS thin films by Successive Ionic Layer Adsorption and Reaction (SILAR) technique by using lead acetate as cationic and thioacetamide as anionic precursor. By using thioacetamide as sulphide source, different chalcogenide thin films were prepared by many workers [19-22]. In chemical bath deposition, film formation takes place when ionic product exceeds the solubility product. This also results into the precipitate formation into the solution and hence sometimes the control over the process was lost. The SILAR method takes care of all these difficulties by immersing substrate into separately placed cationic and anionic precursors and rinsing between every immersion with ion-exchanged water. The aim of this paper is to deposit PbS thin films of different thicknesses at room temperature (300 K) by SILAR method and to study their structural, optical, and electrical properties. Analyzing X-ray diffraction pattern, crystal structure of films and grain size were estimated.

2. Experimental details

2.1. Substrate cleaning :

The important thing before the deposition of films is the careful cleaning of the substrates. As the adherence of the film has a direct bearing on the cleanliness of the substrate, above procedure was adopted, while cleaning the substrates. The slides were washed with liquid detergent and then boiled in conc. chromic acid (0.5 M) for 2 hours and then kept in it for 48 hours. The substrates are then washed with double distilled water. Finally, the substrates are dried using AR grade acetone before use.

2.2. PbS film formation :

The SILAR involves an alternate immersion of the substrate in a solution containing a soluble salt of the cation of the compound to be grown and then in a solution containing a soluble salt of the anion of the compound to be grown. The substrate supporting the growing film is rinsed in high purity deionized water after each immersion. The deposition of PbS thin films on glass slides at room temperature was achieved using 100 ml of 0.01 M lead acetate as cationic and 100 ml of 0.01 M thioacetamide as anionic precursor solution. The pH of thioacetamide solution was adjusted to 12 by adding ammonia in it. The rinsing and immersion time periods were experimentally optimized to get good quality film. The cleaned glass substrates were immersed in lead acetate for 20s, where Pb^{2+}

ions get adsorbed on the substrate. The substrate was then rinsed with deionized water for 30s to remove loosely attached Pb^{2+} ions from the substrate. The rinsed substrate was then immersed in thioacetamide solution for 20s, where S^{2-} ions were adsorbed and reacted with Pb^{2+} ions to grow PbS on the substrate. The unreacted ions were again removed by rinsing the substrate in deionized water for 30s. Adsorption, reaction and rinsing times in SILAR were optimized by varying number of deposition cycles to get good quality PbS thin films. Thus, single deposition cycle consists of 20s adsorption of Pb^{2+} ions, 30s rinsing in water, 20s adsorption and reaction of S^{2-} ions with preadsorbed Pb^{2+} ions on the substrate and 30s rinsing with water. By repeating such deposition cycles the preparative parameters for the room temperature (300 K) deposition of PbS thin films are summarized in Table 1.

Table 1. Optimized preparative parameters for the room temperature deposition of PbS thin films.

| Parameters	Precursors solutions	
	Lead acetate	Thioacetamide
Concentration (M)	0.01	0.01
pH	~5	~12
Immersion time (second)	20	20
Rinsing time (second)	30	30

2.3. Characterization of PbS films :

The average thickness of the film was measured by the gravimetric and Fizzau's method. The two-point dc probe method of dark electrical resistivity was used to study the variation of resistivity with temperature. The copper block was used as a sample holder and chromel–alumel thermocouple was used to measure the temperature. The area of the film (0.5 cm^2) was defined and silver paste was applied to ensure good ohmic contact to PbS films. For the measurement of resistivity, a constant voltage of 16 V was applied across the sample through a transistorized power supply unit (TPSU) and the current was noted using a digital (Keithley) nanoammeter in the temperature range 303–480 K. The structural studies were carried out using Philips PW 1710, diffractometer, with Cu-Ka radiation having wavelength 1.5405 A°. The optical characteristics were studied using Hitachi 330 spectrophotometer to find band gap energy. Using JSM-6360 scanning electron microscope carried out the microstructural studies.

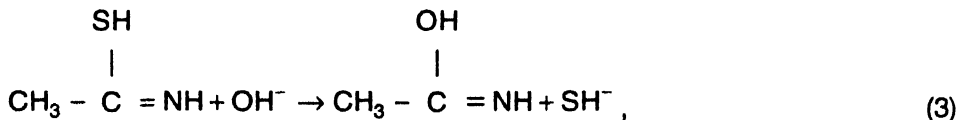## 3. Results and discussion

3.1 Reaction Mechanism :

The SILAR is based on sequential reaction at the substrate surface. The formation of PbS may involve following steps. When the substrate was immersed into cationic precursor where Pb^{2+} ions get adsorbed on to the substrate surface.

$$Pb(CH_3COO)_2 \rightarrow Pb^{2+} + 2CH_3COO^-, \tag{1}$$
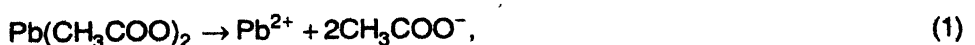
After rinsing in deionised water, substrate was immersed into anionic precursor where Pb^{2+} ions react with S^{2-} to give PbS, which can be explained by using tautomeric form of thioacetamide:

$$
\begin{array}{cc}
S & SH \\
\parallel & \vert \\
CH_3 - C - NH_2 \rightarrow CH_3 - C = NH
\end{array}
\tag{2}
$$

In alkaline medium,

$$
\begin{array}{cc}
SH & OH \\
\vert & \vert \\
CH_3 - C = NH + OH^- \rightarrow CH_3 - C = NH + SH^-,
\end{array}
\tag{3}
$$

$$
SH^- + OH^- \rightarrow S^{2-} + H_2O,
\tag{4}
$$

$$
Pb^{2+} + S^{2-} \rightarrow PbS \downarrow .
\tag{5}
$$

Using optimized conditions and by changing number of SILAR cycles, the films having thicknesses 38 to 189 nm were prepared. The films with number of SILAR deposition cycles less than 50 were discontinuous and therefore number of cycles was taken more than 50. Figure 1 shows variation of film thickness with number of SILAR deposition cycles.
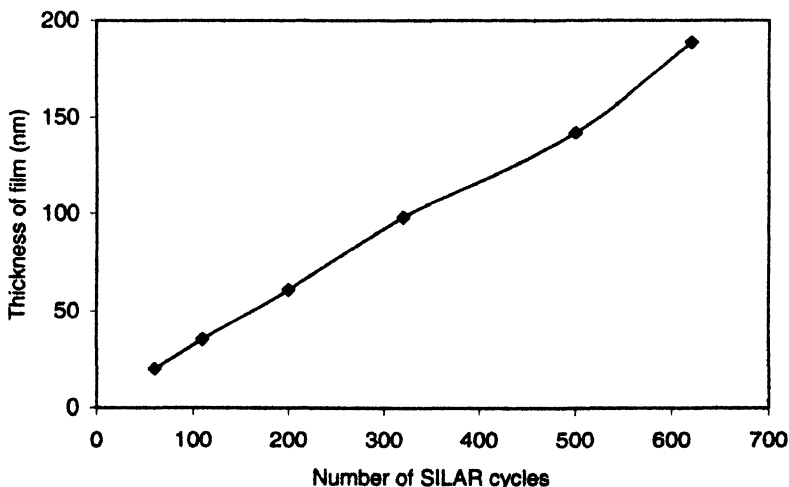

Figure 1. Variation of PbS film thickness with number of deposition cycles.

3.2. XRD studies :

Structural identification of PbS films was carried out with X-ray diffraction in the range of angle 2θ between 10 to 100°. Figure 2 shows the XRD results for PbS thin films, which

were nanocrystalline in nature. The observed broad hump in XRD pattern is due to amorphous glass substrate. The comparison of XRD data with standard ASTM data (JCPDS card 5-592) is given in Table 2, which confirms cubic phase (galena) of PbS. The well defined (111), (200), (220), (311) and (222) peaks were observed in XRD pattern.
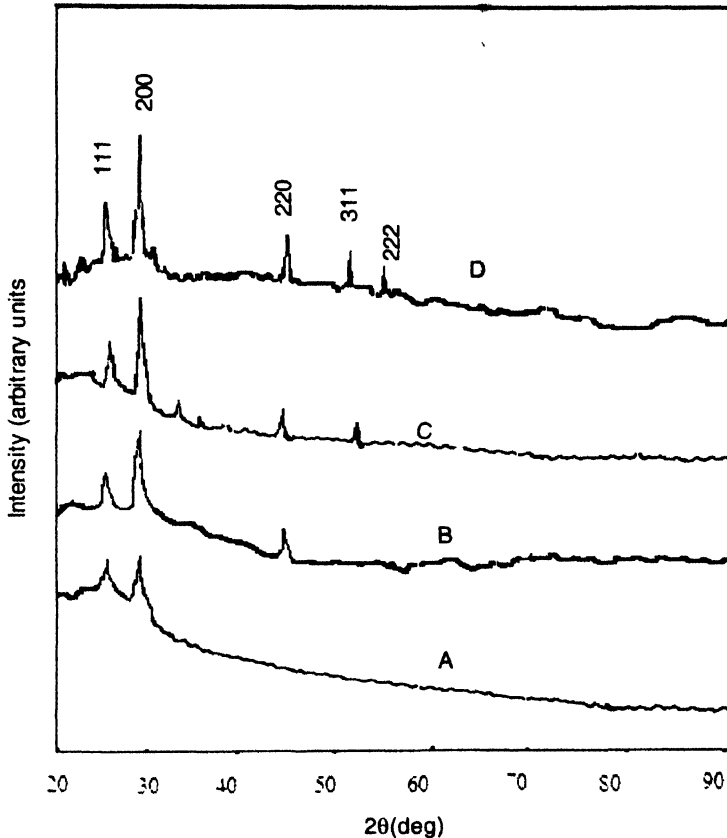
Figure 2. X-Ray diffraction patterns of PbS thin film of different thicknesses: (A) 55 nm; (B) 72 nm ; (C) 96 nm and (D) 189 nm.

The average crystallite size of PbS in the film was determined from the line (200) by using Scherrer formula [23]:

$$d = \lambda / \beta \cos\theta,$$ (6)

where λ is the wavelength used (1.54 A°); β is the angular line width at half maximum intensity in radians; θ is the Bragg's angle. Figure 3 shows variation of grain size with film thickness.

3.3. Resistivity studies :

The dark electrical resistivity of PbS films was studied in the temperature range 303 to 480K using dc two-point probe method. Figure 4 shows the variation of log of resistivity

Table 2. Comparison of crystallographic data for PbS thin films with the JCPDS card 5-592.

Standard data		Observed d (A^0) values for PbS film			
d (A^0)	hkl	Thickness 55 nm	Thickness 72 nm	Thickness 96 nm	Thickness 189 nm
3.429	111	3.431	3.426	3.431	3.428
2.969	200	2.963	2.976	2.978	2.971
2.099	220	–	2.091	2.103	2.095
1.790	311	–	–	1.788	1.789
1.714	222	–	–	–	1.712
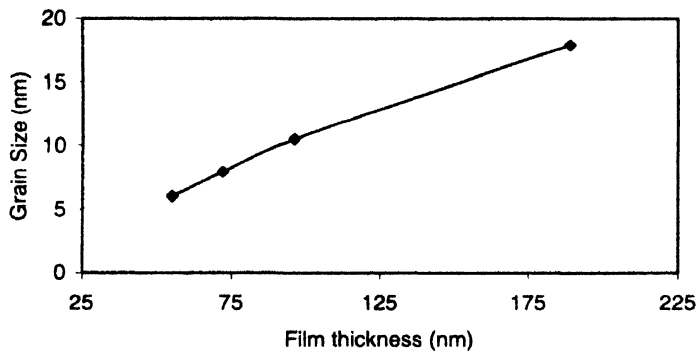
Figure 3. Variation of grain size with film thickness of PbS.

(log ρ) with reciprocal of temperature (1/T) x 10^3. It is seen that resistivity decreases with temperature indicating semiconducting nature of films. The electrical resistivity of
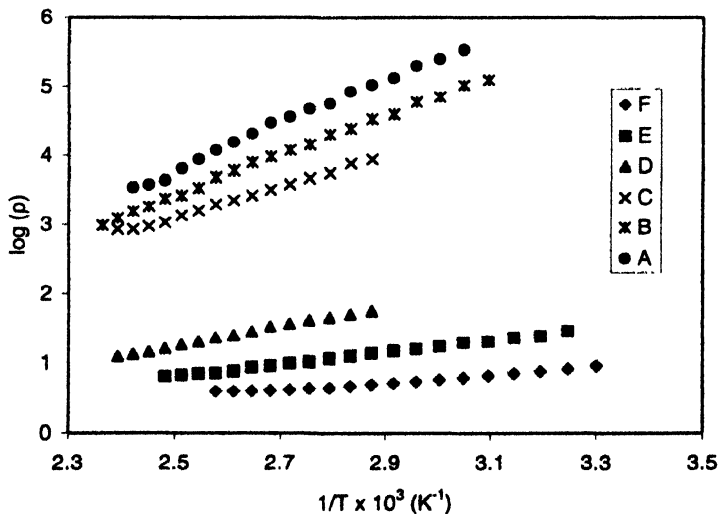
Figure 4. Variation of log (ρ) vs. 1/T x 10^3 (K^{-1}) for PbS films with different thicknesses: (A) 38 nm; (B) 55 nm; (C) 72nm ; (D) 96nm ; (E) 142nm and (F) 189nm.

nanocrystalline material is expected to be higher than in the corresponding coarse-grained polycrystalline materials [24]. The thermal activation energy was calculated using the relation

$$\rho = \rho_0 \exp\left(E_0/KT\right),\tag{7}$$
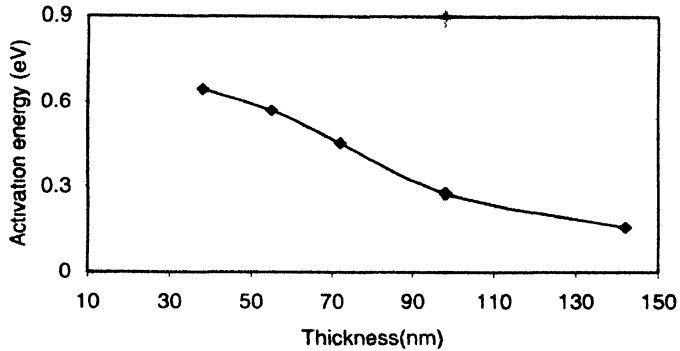
Figure 5. Variation of activation energy of PbS with film thickness.

where, ρ is resistivity at temperature T, ρ_0 is a constant, K is Boltzmann constant (8.62×10^{-5} eV/K) and E_0 is the activation energy required for conduction. Figure 5 shows variation in activation energy from 0.64 to 0.11 eV as thickness changes from 38 to 189nm. These observations may be due to size effects that are arising because of quantum confinement of charge carriers within the particles. Several workers reported the decrease in activation energy with increase in grain size [25,26].
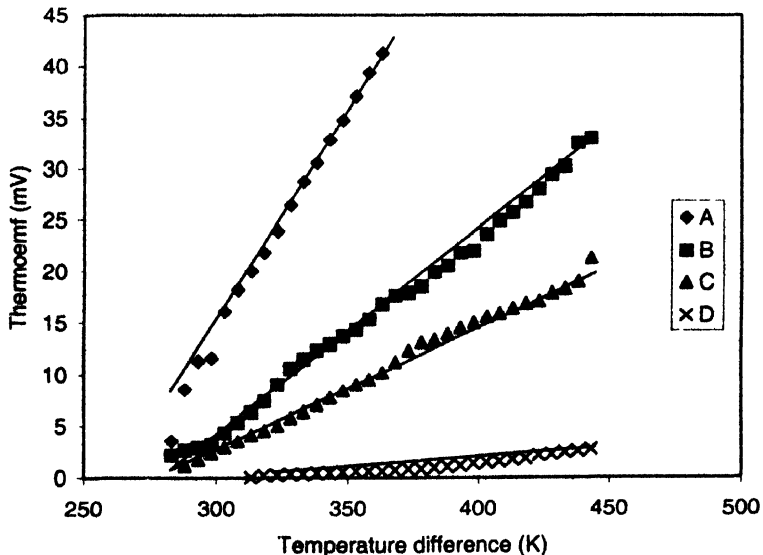

Figure 6. Variation of thermoemf and temperature difference of PbS film with different thicknesses: (A) 55 nm; (B) 96 nm; (C) 142 nm and (D) 189 nm.

3.4. Thermoemf measurements :

Figure 6 shows the variation of thermoemf with temperature difference for PbS films of different thicknesses. From the thermoemf measurement, it was observed that the polarity of thermally generated voltage at the cold end is positive, indicating that the films are of p-type. Increase in thermoemf with increasing film thickness is attributed to the decrease in electrical resistivity caused by increase in grain size.

3.5. SEM studies :

The SEM of the PbS thin films of thicknesses 55, 96, 142 and189nm deposited on glass substrate was examined (Figure 7). The surface of the film is smooth and well covering to the glass substrate. The grains are very small with unequal size and shape; also their grain boundaries are not well defined. Also they reveal that the grain sizes of the films are increased with thickness. Particulate can always be seen on the film surfaces.
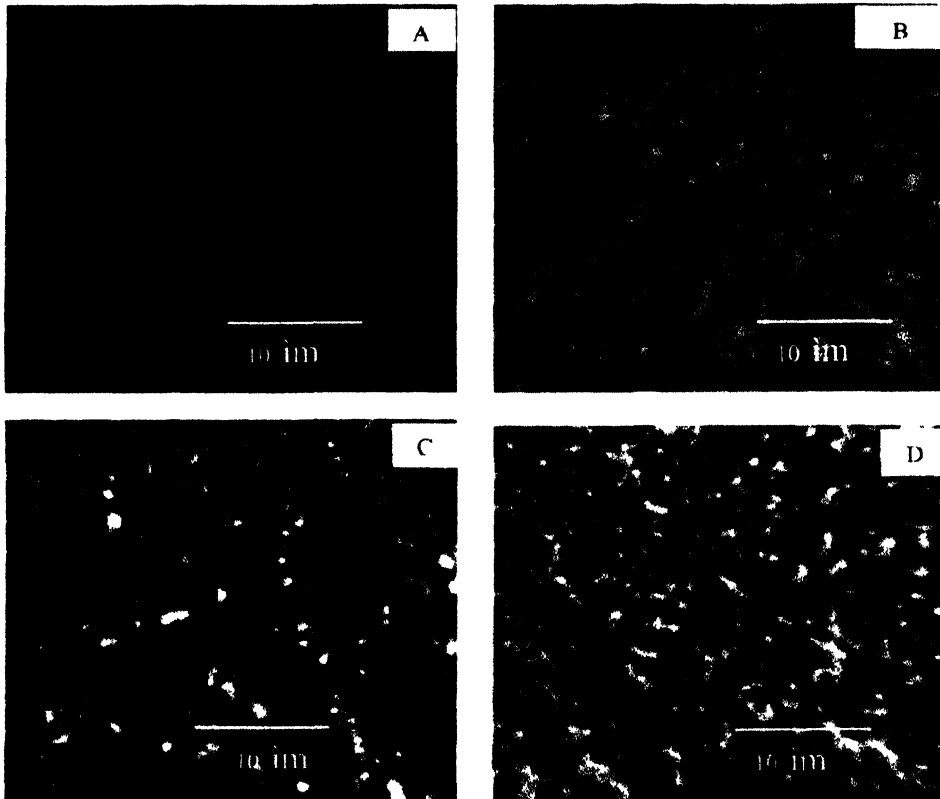
Figure 7. SEM images of PbS film of thicknesses: (A) 55 nm; (B) 96 nm; (C) 142nm and (D) 189nm.

3.6. Optical absorption :

The optical absorption of PbS thin films was studied in the wavelength range of 300 to 850 nm and the variation of optical density (αt) with wavelength (λ) is shown in the
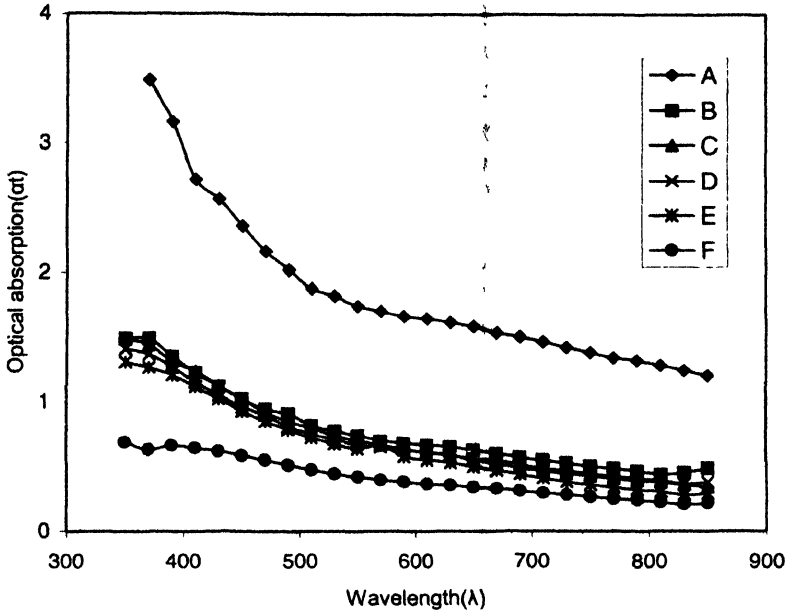
Figure 8. Plot of optical absorption (αt) *vs.* wavelength for PbS films with different thicknesses: (A) 38 nm, (B) 55 nm; (C) 72 nm ; (D) 96 nm ; (E) 142 nm and (F) 189 nm.

Figure 8. All the films show higher absorption on the shorter wavelength side. The nature of the transition (direct or indirect) is determined by using the relation

$$\alpha = \frac{A\left(h\upsilon - E_g\right)^n}{h\upsilon} \qquad (8)$$

where $h\upsilon$ is the photon energy, E_g is the band gap energy, A and n are constants. For allowed direct transitions, $n = \frac{1}{2}$ and for allowed indirect transitions, $n = 2$. The plots of $(\alpha h\upsilon)^2$ versus $h\upsilon$ were shown in Figure 9 for PbS films having different thicknesses. Since the variation of $(\alpha h\upsilon)^2$ with $h\upsilon$ for PbS films is a straight line indicating that the involved transition is direct one. Band gap energy, E_g was determined by extrapolating the straight-line portion to the energy axis for zero adsorption coefficient (α). Figure 10 shows variation in optical band gap energy from 1.86 to 2.36 eV with thickness from 189 to 38
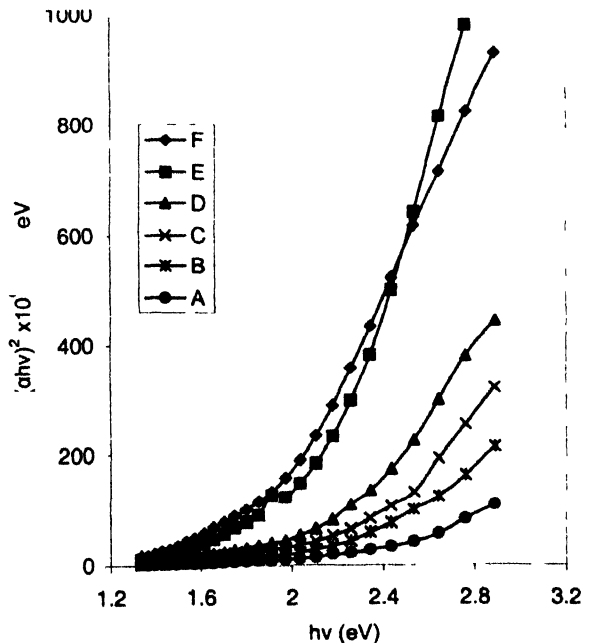

Figure 9. Plot of $(\alpha h\upsilon)^2$ *vs.* $h\upsilon$ for PbS films with different thicknesses: (A) 38 nm; (B) 55 nm; (C) 72 nm; (D) 96 nm ; (E) 142 nm and (F) 189 nm.

nm. This is attributed to the crystallite size-dependant properties of the energy band gap. Similar 'blue/red shift' in band gap energy 'E_g' values for the films with smaller thickness and/or crystallite sizes have been reported for chemically deposited thin films [27,28].
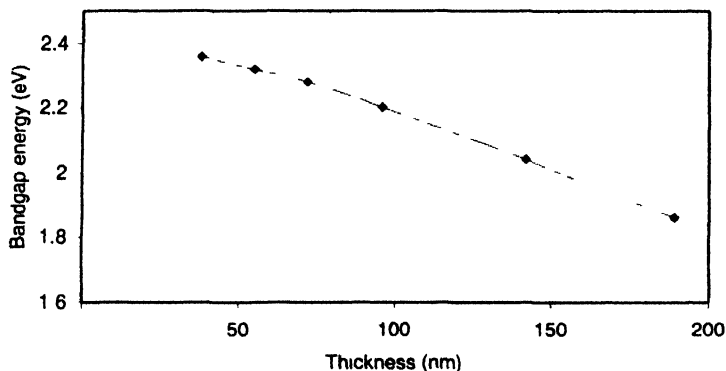

Figure 10. Variation of optical band gap energy, E_g, with film thickness.

4. Conclusions

Growth of nanostructured PbS thin films at low temperature by a simple chemical method, Successive Ionic Layer Adsorption and Reaction (SILAR) is possible. An XRD study shows nanocrystalline structure with cubic phase (galena). Optical studies show that the absorption spectrum is due to transition from one band to another and is mainly caused by allowed direct transitions. The optical band gap energy varies from 1.86 to 2.36 eV with thickness. The electrical resistivity and therefore activation energy are observed to be thickness dependent. The results of XRD and SEM show that the deposited PbS film consists of nano-sized grains (6–18 nm), and the grain size increases with increasing film thickness.

Acknowledgment

References

[1] B R Chackraborty, B Roy, R Bhattacharya and A K Datta *J. Phys. Chem. Solids* **41** 913 (1980)

[2] Y Wang and N Herron *J. Phys. Chem.* **95** 525(1991)

[3] R Resh, G friedbacher, M Grasserbauer, T Kannianinen, S Lindross, M Leskela and L Ninisto *Appl Surf. Sci.* **120** 51 (1997)

[4] J J Valenzuela-Jauregui, R Ramirez-Bon, A Mendoza-Galvan and M Sotelo-Lerma *Thin Solid Films* **441** 104 (2003)

[5] I Pop, C Nascu, V Ionescu, E Indrea and I Bratu *Thin Solid Films* **307** 240 (1997)

[6] C Nascu, V Vomir, I Pop, V Ionescu and R Grecu *Mater.Sci.Engg.* **B841** 235 (1996)

[7] K K Nanda and S N Shau *Appl.Phys. Lett.***79** 2743 (2001)

[8] S Watanabe and Y Mita *J. Electrochem.Soc.***116** 989 (1969)

[9] I Pintitie, E Pentia, D Petre, L Pintilie and T Btila *J.Appl. Phys.***78-3** 1713 (1995)

[10] K M Gadave, S A Jodgauri and C D Lokhande *Thin Solid Films* **245** 7 (1994)

[11] N Sharma, D K Pandya, H K Seghal and K L Chopra *Thin Solid Films* **59** 157 (1979)

[12] H N Acharya and H N Bose *Phys. Stat. Sol.* K-43 (1973)

[13] P K Nair and M T S Nair *J. Phys.* **D 23** 150 (1990)

[14] T P Sharma, R Kumar, G Jain and S C Mishra *Indian J. Pure Appl. Phys.* **29** 583 (1991)

[15] M Ristov, G J Sinadinovskt and I Grovdanov *Thin Solid Films* **126** 63 (1985)

[16] Y F Nicolau *Appl. Surf. Sci.* **22** 1061 (1985)

[17] Y F Nicolau and J C Menard *J. Crystal Growth* **92** 128 (1988)

[18] R Ortega-Borges and D Lincot *J. Electrochem. Soc.* **140** 3464 (1993)

[19] P Parmanik, P K Basu and S Biswas *Thin Solid Films* **150** 269 (1987)

[20] S Biswas, A Mandal, D Mukherjee and P Parmanik *J. Electrochem. Soc.* **133(1)** 48 (1986)

[21] P K Basu and P Parmanik *J. Mater.Sci.Lett.* **5** 1216 (1986)

[22] P Parmanik, and S Biswas *J. Solid State Chem.* **65** 145 (1986)

[23] B D Cullity *Elements of X-ray Diffraction* (MA : Addition-Wesley) p102 (1978)

[24] P K Nair, V M Garcia, A M Fernadez, H S Ruiz and M T S Nair *J.Phys.* **D 24** 441 (1991)

[25] C A Estarde, E A Myers, R A Zingaro, D C Dufner, P K Nair and M T S Nair *Heteroatom Chem.* **6** 349 (1995)

[26] S S Kale and C D Lokhande *Mater. Chem. Phys.* **62** 103 (2000)

[27] G Hodes, A Albu-Yaran, F Decker and P Matsuke *Phys. Rev.* **B 36** 4215 (1987)

[28] G Hodes *Israel J. Chem.* **33** 95 (1993)